

Linear augmented-Slater-type-orbital method for electronic-structure calculations.

IV. $5d$ - $5d$ alloys

R. E. Watson, J. W. Davenport, and M. Weinert

Physics Department, Brookhaven National Laboratory, Upton, New York 11973

(Received 8 August 1986)

We have used local-density calculations to study a series of transition-metal compounds which are isoelectronic with rhenium: WOs, TaIr, and HfPt. The calculations were carried out for two different crystal structures, CsCl and CuAuI. We find that the heats of formation are in reasonable accord with experiment and increase with the difference in atomic number. We also find a crossover in crystal structure from CuAuI for OsW and TaIr to CsCl for HfPt, which is consistent with experiment. Charge transfer in the series was investigated by Mulliken populations and by Wigner-Seitz sphere counts. These were compared with the shifts in contact density and core-level binding energy. We find that the change in contact density is consistent with electronegativity arguments and involves both changes in s count and d (or at least non- s) screening contributions. The changes in (initial-state) core-level binding energy do not follow the same trend—in fact, for two of the compounds, the change in binding energy relative to the Fermi energy has the same sign for the two constituents.

I. INTRODUCTION

The alloys of the $5d$ transition-metal elements, Lu—Au, are an interesting sequence to study. Though relativistic effects must be accounted for, these systems may be considered to be prototypes of transition-metal alloying: They avoid the complications due to magnetism encountered in the $3d$ row and avoid Pd and Ag in the $4d$ row, these atoms being somewhat unusual in having d bands which lie abnormally low with respect to the non- d bands. Calculations for the heats of formation and for charge transfer will be reported for the compounds PtHf, IrTa, and OsW in this paper. There are experimental heat of formation data for the first two systems and a semiquantitative value can be inferred for OsW from its phase diagram. The three systems have a common number of conduction electrons and hence, in a “rigid-band” view, would be deemed similar. This is not the case. PtHf contracts upon compound formation (i.e., the molecular volume in the compound is measurably smaller than the sum of the elemental metallic volumes), and this is often taken to be an indication of ionic bonding character. IrTa does not display such a contradiction and forms in another crystal structure, while 50-50 OsW is a two-phase material, one being the terminal solution phase of hcp Os, the other a W-rich brittle σ phase.

The calculations employ density-functional theory and the recently developed linear augmented-Slater-type-orbital method^{1,2} (LASTO) to obtain total energies for the compounds. (See Appendix A.) A major motivation of the present paper is the exploration of the applicability of LASTO to such compounds. We include relativistic effects in the scalar relativistic approximation, i.e., spin-orbit coupling is neglected in the conduction bands (though not in the core) but all other relativistic effects are included. Muffin-tin potentials are employed.

The LASTO method has the virtue of retaining a physi-

cally appealing and interpretable labeling of the orbital basis, while at the same time permitting systematic improvement in both the basis and the potential by the inclusion of more than one STO per quantum number l at a site. Minimum basis set LASTO calculations will be exploited here in order to obtain molecular populations employing the Mulliken³ and a modified Mulliken scheme⁴ (see Appendix B). These provide a measure of the charge residing in orbitals *centered* on a given site, even if their tails extend into other sites. This is an intuitively appealing measure of the electron charge associated with a constituent atom. The problem, of course, is that the orbitals on different sites are not orthogonal to one another and this nonorthogonality must be dealt with. The Mulliken scheme provides one method for dealing with this which is particularly convenient to employ with the present band-theory results. The results of any such scheme depend on the *choice* of the STO used in the calculations. The STO employed here were chosen to optimize the total energies of the elemental metals. A more traditional approach to estimating site charge counts is to draw Wigner-Seitz cells (or Wigner-Seitz spheres) around individual sites and to integrate the electron density inside. For systems with more than a single species of atomic sites the resulting charge counts depend on the *choice* of site volumes. In addition, evidence will be seen that the wave-function tails, which complicate the molecular population counts, also complicate the Wigner-Seitz cell counts.

The plan of the paper is as follows. Section II discusses the total-energy calculations. Linearized augmented-plane-wave (LAPW) as well as LASTO results will be reported for the heats of formation of the compounds in the CsCl and CuAuI structures. The two sets of calculated heats are in essential agreement with one another and with the experimentally observed structural trend. Section III follows with the measures of charge transfer. In addition

to the two types of measure discussed above, two quantities relevant to experiment will also be considered. These are the shifts in core-level one-electron energies (i.e., the "initial-state" contributions to core-level photoemission) and the charge contact densities at the nucleus. The latter is the quantity entering Mössbauer isomer shift measurements, and this is particularly relevant to the 5*d* elements since Ta, W, Os, Ir, Pt (and Au) have nuclei with the appropriate nuclear transitions for such measurements. Some features of the experimental contact density shifts, seen for these elements as dilute impurities, are reflected in the results for 50-50 compounds obtained here. While measures of charge transfer are substantially affected by the complications alluded to above, meaningful patterns do occur in the present results.

II. HEATS OF FORMATION

A heat of formation is defined by taking the difference between the total energy obtained for the compound and the sum of the elemental metal total energies. The STO, which yielded² the optimum energies for the elemental metals, were employed in the compounds as were the radial integration meshes used for the elements. Muffin-tin sphere radii R_S corresponding to touching spheres for the elements in the bcc structure were used. The calculations were done at fixed lattice constants which, for PtHf and IrTa, were based on molecular volumes available from experimental crystallographic data for these systems in the vicinity of 50-50 concentration. The resulting volumes are 249.19 and 212.74 a.u.³ for PtHf and IrTa, respectively. Because there are no data for OsW, the sum of the elemental volumes were assigned to the compound. In viewing what follows it should be remembered that PtHf has been reported in the CsCl structure and IrTa in the CuAuI; although at slightly off exact 50-50 stoichiometry in both cases. The CuAuI structure is an *ABAB* stacking of fcc (100) planes. In the ideal structure the *A-A* distance is just *a*, the cubic lattice constant. Usually there is a tetragonal distortion along the stacking direction and for example in TaIr $c/a = 0.968$. In our calculations we have used the same c/a ratio for the other compounds. For $c/a = 1/\sqrt{2}$ the structure becomes identical with CsCl. As noted above, no compounds form in the vicinity of 50-50 composition in OsW, suggesting that the heats of such ordered 50-50 structures for this system are likely to be small in magnitude and positive (i.e., nonbonding) in sign.

The calculations have been done using sets of special *k* points^{5,6} for which there remains the issue of how small a set suffices. An indication of this is shown in Fig. 1 where the heats of formation,

$$\Delta H \equiv E(AB) - E(A) - E(B), \quad (1)$$

are shown for the three systems in the CsCl structure, where $E(AB)$ is the compound's total energy for some given *k* set and the elemental metal energies $E(A)$ and $E(B)$ have been calculated with fixed (large) *k* sets. The mesh with $\frac{1}{8}$ th Δk intervals is the 4-point mesh listed in Chadi and Cohen⁵ while the $\frac{1}{16}$ th and $\frac{1}{32}$ nd, for example, involve meshes of 20 and 120 *k* points, respectively. Al-

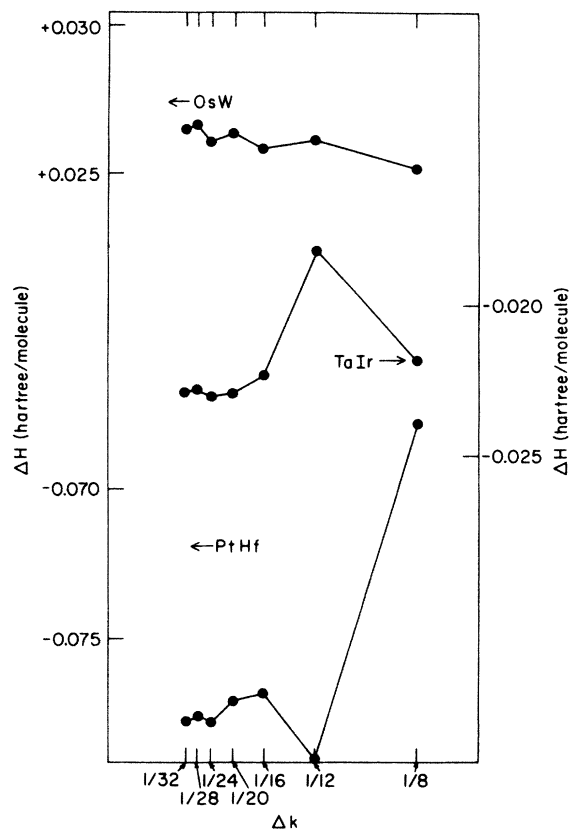


FIG. 1. Heat of formation of OsW, TaIr, and PtHf in the CsCl structure versus Δk —the mesh spacing for the Brillouin-zone sampling. $\Delta k = \frac{1}{8}$ corresponds to 4 special points and $\Delta k = \frac{1}{32}$ corresponds to 120.

though the three systems have a common electron-to-atom ratio, their band structures are sufficiently different so that the evolution in calculated total energies, as a function of improved *k* sampling, differ markedly. Similar results are shown for TaIr in both the CsCl and CuAuI structures in Fig. 2. The CuAuI structure is calculated to be the more stable, consistent with experiment, and in no case is the issue in doubt. Being of lower symmetry (tetragonal versus cubic) the CuAuI structure requires a *k* sampling over a larger slice of the Brillouin zone and, as a result, the *k* sets are greater. They involve 6, 40, and 196 *k* points for the Δk of $\frac{1}{8}$, $\frac{1}{16}$, and $\frac{1}{28}$, respectively. For the compounds considered in this paper, the $\Delta k = \frac{1}{16}$ meshes yield energies which are within one millihartree of the results for much finer meshes (though, having obtained them, the finest mesh results are used here). This is consistent with the results² for the elemental metals.

The calculated heats of formation are summarized in Fig. 3 where, for the majority of cases, LAPW as well as LASTO results are shown. Differences between the two are a measure of the effect of having used minimum basis sets in the LASTO calculations. The differences are slight. The calculations correctly predict the CsCl structure to be the more stable for PtHf, the CuAuI to be so for IrTa, and, as might be presumed from the phase dia-

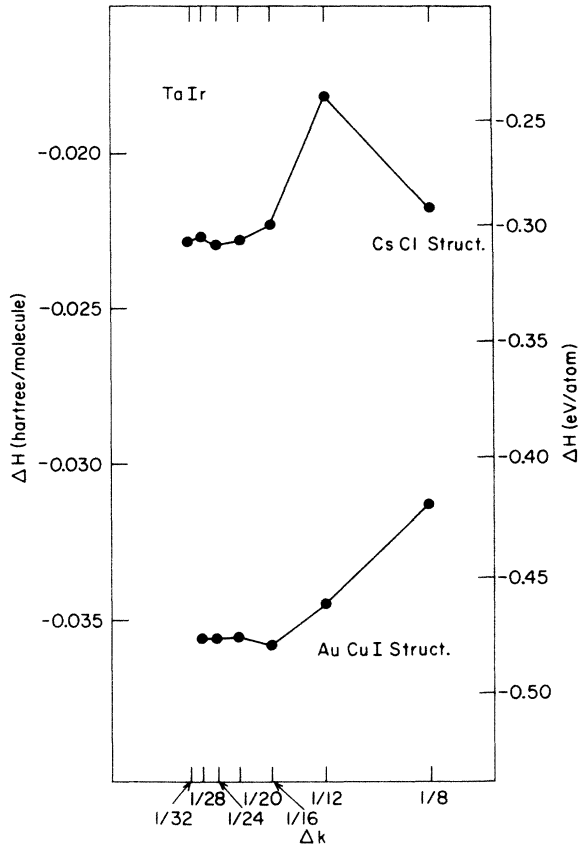


FIG. 2. Heat of formation of TaIr in the CsCl and CuAuI structure versus Δk —the mesh spacing for the Brillouin-zone sampling.

gram behavior, that OsW has small, nonbonding heats in these structures. The experimental ΔH in parentheses, (*), for PtHf is old data whose large magnitude caused problems for an interpolation scheme⁷ based on a simple Friedel *d*-band model. The more recently obtained value,⁸ not in parentheses, is in good accord with the calculations. However, it and the ΔH for TaIr would seem to be inconsistent since linear extrapolation off the two would suggest a substantial bonding for OsW which is contrary to the observed phase diagram. It would appear likely that one of the two experimental values is in error, and granted the agreement with theory for PtHf, the authors would suggest that the problems lie with TaIr. Discrepancies of the scale in question are not unknown for different experimental data for the same alloy system (witness the two values for PtHf): We may be entering an era where band theory, done with sufficient care, provides the more economic means for obtaining ΔH for such compounds.

III. CHARGE TRANSFER

Charge transfer at the Pt, Ir, and Os sites, as measured by the Mulliken, modified Mulliken, and Wigner-Seitz (WS) cell⁹ schemes is indicated in Fig. 4. Charge transfer

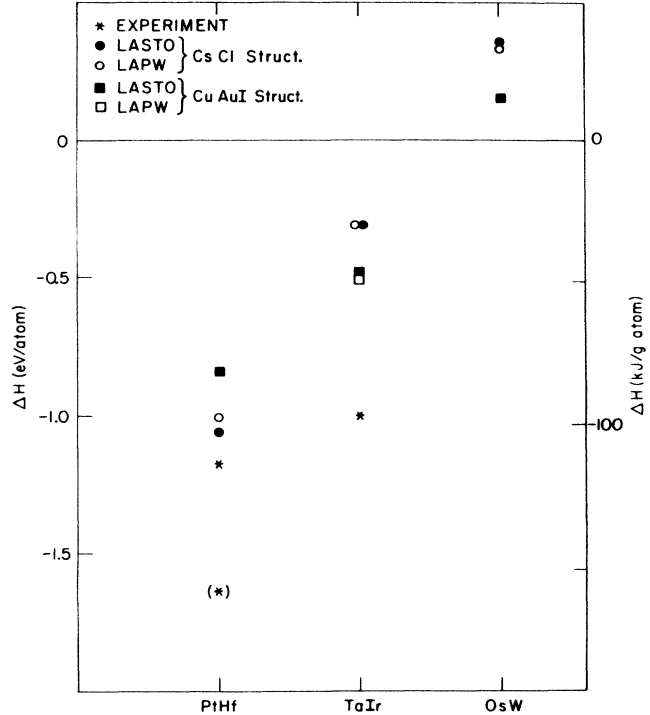


FIG. 3. Heat of formation of OsW, TaIr, and PtHf in the CsCl and CuAuI crystal structures compared to experiment. Calculations were performed both with the LASTO and with the LAPW method. The experimental value in parentheses (*) is older.

at the companion Hf, Ta, and W sites is, of course, equal in magnitude and opposite in sign. It is normally presumed that Pt, Ir, and Os are more electronegative than Hf, Ta, and W and, therefore, that electron charge transfer should be onto the former. However, in addition to the substantial spread in charge transfer counts for a given compound, the WS cell counts and the Mulliken counts for the CuAuI structure indicate charge flow off of Pt, Ir, and Os, contrary to expectations. Some of the spread in the molecular populations (and the dip seen for IrTa relative to the compounds to either side) may be attributed to the Slater orbitals employed in the interstitial region. These orbitals were chosen so as to optimize² the total energies of the elemental metals and the *p* orbitals are particularly diffuse, implying large intersite overlaps and hence large overlap corrections in the molecular populations.

Stranger than any shortcomings in the molecular populations, is the tendency for the WS cell counts to go the "wrong" way. The reason for this is suggested in Fig. 5. While only the tails of *s*-, *p*-, and *d*-like orbitals are used in the interstitial region, the LASTO calculations, like the LAPW, involve eigenfunctions for *l* values ranging from 0 to 8 *inside* the atomic spheres. The high-*l* components are necessary for boundary conditions on the sphere surfaces and are a real part of the charge density. (They must be included in the calculations if accurate total energies are to be obtained by the LASTO or other augmented

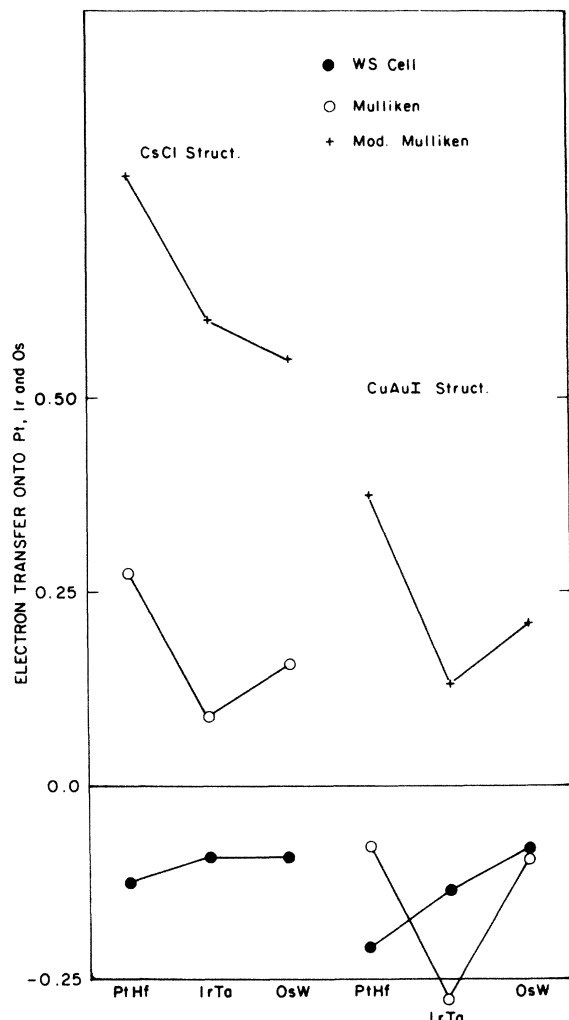


FIG. 4. Charge transfer to Pt, Ir, or Os as measured by the Wigner-Seitz, Mulliken, and modified Mulliken populations for OsW, TaIr, and PtHf in the CsCl and CuAuI crystal structures.

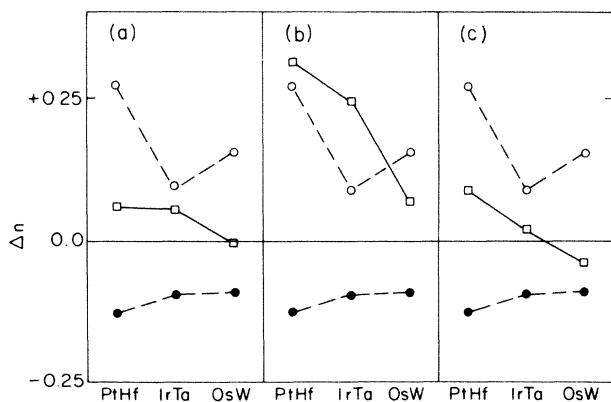


FIG. 5. Charge transfer to Pt, Ir, or Os as measured by various Wigner-Seitz populations (\square). For convenience the Mulliken (\circ) and Wigner-Seitz (\bullet) populations from Fig. 4 have been included in each figure. (a) Sum of s , p , and d charges for a calculation which included $l \leq 8$; (b) sum of s , p , and d charges plus sum of charges for $l = 3-8$ on the nearest neighbor; (c) sum of s , p , and d charges for a calculation which included $l \leq 2$ only. These results are for the CsCl structure.

methods.) In Fig. 5(a), the charge transfer associated with the s , p , and d components *only* of the WS cell densities for the CsCl structures are shown. We notice that except for Os the summed s , p , and d charge changes are *opposite in sign* to the total charge transfer. This is also true for the electropositive W, Ta, and Hf which are not shown. In other words, the sign of the charge flow is determined by the high- l components. Now, these may be viewed as being the *tails* of s , p , and d orbitals centered on neighboring sites and, as such, might well be attributed to those neighboring sites. In the CsCl, but not the CuAuI structure, all nearest-neighbor sites are populated by unlike atoms and, if one attributes the tails to these nearest-neighbor sites alone, then one can employ the integration within WS cells to obtain population counts consisting of the s , p , plus d terms in a sphere *plus* the high- l in *unlike spheres*. The result is plotted in Fig. 5(b). Done in this way, the WS cell results are in semiquantitative agreement with the Mulliken population changes. In both cases, the treatment of the s , p , and d electron tails, in regions off the site they are centered on, substantially affects any estimate of charge transfer. The results of band calculations where the l were limited to 0, 1, and 2, in the atomic spheres, appear in Fig. 5(c). These are in essential agreement with the results of Fig. 5(a); that is, the charge transfer associated with the $l = 0, 1$, and 2 components in the WS spheres is independent of whether the high- l components are carried in the calculation. However, the total charge transfer is in large part controlled by these higher- l components.

Individual s , p , and d WS cell electron count changes are plotted in Fig. 6 for both the CsCl and the CuAuI structures. It is seen that the separate s , p , and d transfers are of the same order. Except for the crossovers in Δn_d for PtHf, there is the tendency for increasing individual Δn values on going from OsW to IrTa and, in turn, PtHf. This trend is consistent with the traditional view that the electronegativity differences, hence charge

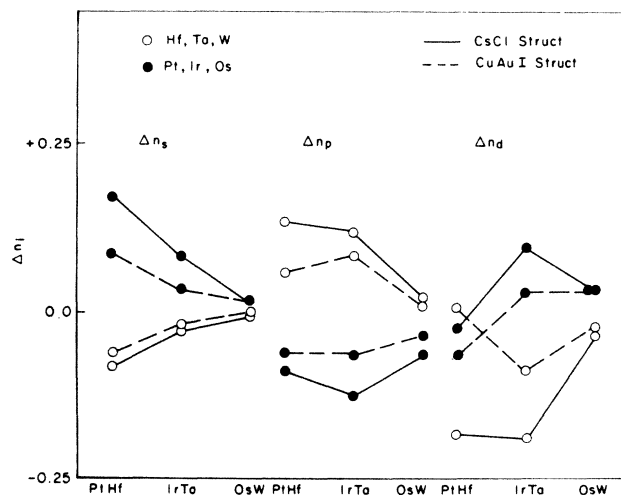


FIG. 6. Charge transfer as measured by the s , p , and d Wigner-Seitz populations.

transfer and bonding, increase across the sequence. This pattern is less clear in the total charge transfer counts because of the high- l components and the question of how to deal with them, as discussed above. The results displayed in Fig. 6 suggest that, shell by shell, the bonding in the CsCl structure is the more ionic, i.e., the charge transfer greater, than in the CuAuI despite the fact that there is no evidence for this when the high- l components are added in. This apparent difference in ionicity may be associated with the fact that all eight nearest neighbors in the CsCl structure are unlike atoms, whereas only eight of the twelve nearest neighbors in the CuAuI structure are unlike.

Individual shell orbital population changes are compared with those of the WS counts for the CsCl structure in Fig. 7(a). It should be remembered that the entire charge transfer resides in orbital population terms whereas there are the high- l components to be added to the WS cell values. Despite this, the trends in the Δn are remarkably alike with semiquantitative agreement for the d terms, somewhat poorer for the s and worst for the p . This correlates with the spatial extent of the STO's; the p , being the most diffuse, has charge transfer counts which are the most affected by tailing. Greater discrepancies are to be seen in the CuAuI structure results in Fig. 7(b).

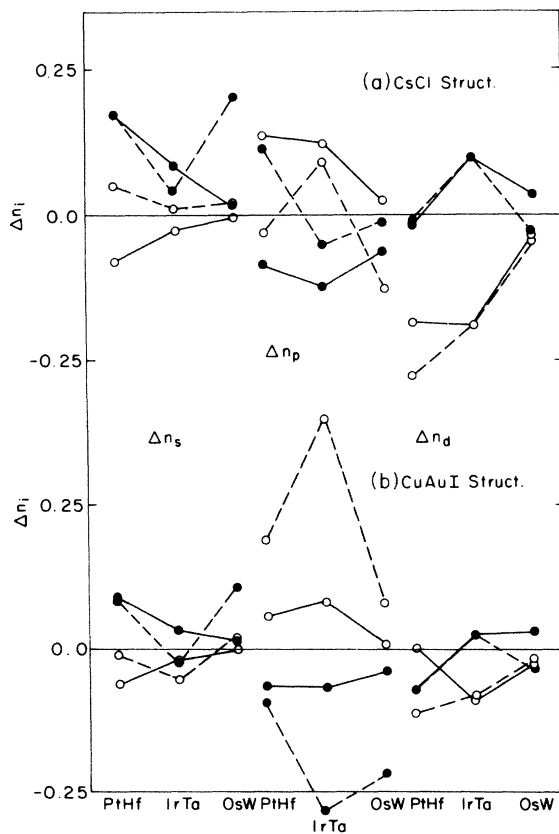


FIG. 7. Charge transfer as measured by the s , p , and d Mulliken populations (dashed lines) compared with the Wigner-Seitz populations (solid lines) for (a) CsCl structure and (b) CuAuI structure. Solid circles are for Pt, Ir, and Os and open circles are for Hf, Ta, and W.

A simple argument can be made concerning the direction of d transfer provided that only d bands, occupied only by d orbitals, are involved in hybridization.¹⁰ Hybridization involves mixing unoccupied wave-function character into occupied bands, thereby increasing the occupation of the former type of wave function while reducing the occupation of orbital character initially in the occupied bands. A metal with less-filled bands has more unoccupied d -band character available for hybridizing into the alloy bands and less to lose by alloying. This would suggest that Δn_d should be negative for Pt, Ir, and Os and opposite in sign for Hf, Ta, and W. Only Pt obeys¹¹ this (preliminary results for other Pt and Au alloys also show Pt and Au following such a trend). The situation is obviously more complicated, and part of the problem involves differentiating between band occupancy and orbital occupancy—there is, for example, significant non- d character hybridized into the occupied d bands of the elemental metals. The d bands of Pt have been known for some time to be filled when Pt is alloyed to elements to the left of it in the Periodic Table and, if it were not for the d orbital depletion, Coulomb energy terms would make such band filling energetically impossible. From Figs. 5–7 it would appear that the balance of s , p , and d transfer terms is quite complex and depends on the crystal structure involved.

IV. CORE-LEVEL SHIFTS

The atomic cores are treated self-consistently in the course of the band calculation and their one-electron energies ϵ_i , as well as the Fermi levels ϵ_F , are calculated. Now, the quantity $\epsilon_i - \epsilon_F$ would be the experimental photoemission energy if it were not for the screening of the final-state hole associated with the photoemission process. Of interest are the chemical effects associated with the photoemission shift, $\Delta(\epsilon_i - \epsilon_F)$, upon alloying. Since the final-state screening is substantial, changes in the relaxation may mask $\Delta(\epsilon_i - \epsilon_F)$ such that neither the sign nor the magnitude is obvious. Crudely speaking, there are three contributions to $\Delta(\epsilon_i - \epsilon_F)$: first, there is the shift in the Fermi level with alloying; second, there are shifts in ϵ_i due to any on-site changes in the valence-electron charge density; and third, there are the shifts due to off-site effects. It is difficult to separate the three terms in a satisfactory way. However, we know V_c , the potential at the surface(s) of the atomic spheres separating the atoms from the interstitial region. The quantity $\Delta(\epsilon_i - V_c)$ provides a measure of the level shifts due to on-site chemical effects. It and the $\Delta(\epsilon_i - \epsilon_F)$ are plotted for the $4f_{7/2}$ core electrons in Fig. 8. DasGupta and co-workers have reported¹² level shifts of -0.83 and $+0.17$ eV for Ta and Ir, respectively, for a $\text{Ta}_{0.55}\text{Ir}_{0.45}$ alloy. Presumably it is most appropriate to compare these with the calculated $\Delta(\epsilon_{4f} - \epsilon_F)$ values for the CuAuI structure which is known to occur at the Ir-rich side of 50-50 composition. There is essential agreement between calculation and experiment for Ir, suggesting little contribution from changing final-state screening between the elemental metal and the alloy. In contrast, there is agreement in sign but the calculated value is 0.5 eV smaller in magnitude (and 0.1 eV smaller

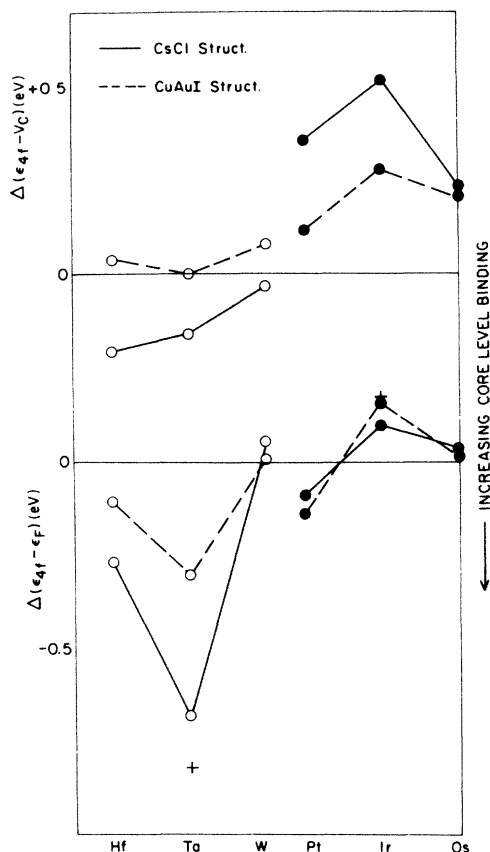


FIG. 8. Core-level shifts as measured by the change in the $4f_{7/2}$ eigenvalue relative to the Fermi level and by the change in eigenvalue relative to the Coulomb potential at the sphere boundary V_c . + is the experimental result for TaIr from Ref. 12.

for the less-appropriate CsCl structure) for Ta. Since final-state screening reduces the apparent binding energy of a level, the discrepancy would indicate that the final-state screening is less effective in the alloy than it is in elemental Ta. Such observations assume that both the calculations and experiment are of sufficient accuracy.

Consider $\Delta(\epsilon_{4f} - V_c)$ in the figure. Again there is an indication that the CsCl structure is substantially more ionic than the CuAuI. Granted that an increase (decrease) in on-site valence charge causes a decrease (increase) in core-level binding, $\Delta(\epsilon_{4f} - V_c)$ correlates in a semiquantitative way with the Δn_d of Fig. 6. By involving the most compact charge density, any change in the d orbital occupation should have a larger effect on the level shift than an equal Δn in another l component.¹³ The s component should be the next most important, followed by the p and, in turn, the high l . The main discrepancy between the $\Delta(\epsilon_{4f} - V_c)$ and the Δn_d is that the former show larger effects for Pt, Ir, and Os while the Δn_d are larger in magnitude for Hf, Ta, and W. This is, in part, due to contributions from the other charge transfer terms and, in part, due to making reference to V_c , the potential at the atomic sphere radius: Elements such as Hf and Ta have a significantly larger fraction of their d charge outside this radius than do Pt and Ir. While having the virtue of being well

defined, V_c is still not a completely satisfying reference potential.

V. CONTACT DENSITIES

As noted in the Introduction, Ta, W, Os, Ir, Pt, and Au have nuclear γ -ray transitions, allowing isomer shift measurements with the Mössbauer effect. The isomer shift ΔS (mm/s) involves the difference in electron contact density between two samples, a source and an absorber, where

$$\Delta S \text{ (mm/s)} = [0.00608 Z \delta \langle r^2 \rangle \Delta \rho(0)] / E_\gamma \quad (2)$$

Z , $\delta \langle r^2 \rangle$, E_γ , and $\Delta \rho(0)$ are, respectively, the nuclear charge, the change during the nuclear transition in the square of the nuclear radius (10^{-3} fm^2), the γ -ray energy (keV), and the difference in electron density (a_0^{-3}) at the nucleus in the source versus that in the absorber. It should be noted that neither $\delta \langle r^2 \rangle$ nor individual $\rho(0)$ have well-established experimental values. The s (and relativistic $p_{1/2}$) orbitals are nonzero at the nucleus and, therefore, ΔS is a measure of changes in their character. First, there are the changes in s occupancy in the conduction bands, and second, any changes in other valence electron character will affect the screening of the s , hence modifying its contact density. For example, the d orbitals are more compact than the s and an increase in d count will increase d screening, causing the s charge to dilate and have a smaller $\rho(0)$. Thus increases in other valence charge counts look like decreases in the s .

There is considerable experimental ΔS data for the above-listed elements as dilute impurities in transition-metal hosts. As a rule the contact density decreases as an atom is taken from one host to another to the right of it in the Periodic Table. The data have been normalized¹⁴ to obtain

$$\Delta S' \equiv \frac{\Delta S}{Z \delta \langle r^2 \rangle \rho(0) / E_\gamma} \quad (3)$$

where the $\rho(0)$ was a renormalized $6s$ electron contact density. It was possible to fit the data for a sequence of hosts and infer the change in S for a change in host column in the Periodic Table, $\Delta S' / \Delta n$. The resulting $\Delta S' / \Delta n$ varied from being near zero for Ta and W to being large for Pt and Au impurities. The very size of the Pt and Au results was used to argue that there was significant screening due to d transfer which was added to s transfer contributions (which following the argument made above would imply Δn_d to be opposite in sign to Δn_s). The variation in $\Delta S' / \Delta n$ was then taken to imply a variation in the balance of s and d transfer terms on going from the alloying of Ta to that of Au. More recently, Akai and co-workers have considered another problem,¹⁵ namely the isomer shift at a host Fe site due to a nearest-neighbor substituted impurity. Their theoretical results were in agreement with experiment and showed the ΔS at the host Fe sites to faithfully reflect Δn_s alone. The present situation is different than either of the above for it involves the isomer shifts for ordered 50-50 alloys.

Contact densities have been calculated for the elemental metals and for the alloys. The alloy shifts have been normalized, in the spirit of Eq. (3), by forming

$$\Delta\rho' \equiv n_s \Delta\rho(0)/\rho_v(0), \quad (4)$$

where $\Delta\rho_v(0)/n_s$ is the contact density per s electron, as measured with the WS cell counts, in the valence bands of the elemental metal. (WS cell counts have been used, since we are concerned with the amount of s -like charge penetrating into the interior of the atom.) The resulting $\Delta\rho'$ are shown in Fig. 9(a). They indicate increased contact densities for Pt, Ir, and Os and decreases for Hf, Ta, and W. This is consistent with simple electronegativity arguments and with the gross Mulliken populations shown in Fig. 4. It is not consistent with the gross Wigner-Seitz populations, again illustrating that the high- l components should plausibly be assigned to neighboring sites. In fact, the Wigner-Seitz s charges do follow the expected trend. Larger effects, indicating greater ionicity, are again seen for the CsCl structure. Comparison with the normalized experimental data suggests that significantly more charge transfer is involved in the dilute alloys than in the 50-50 compounds treated here.

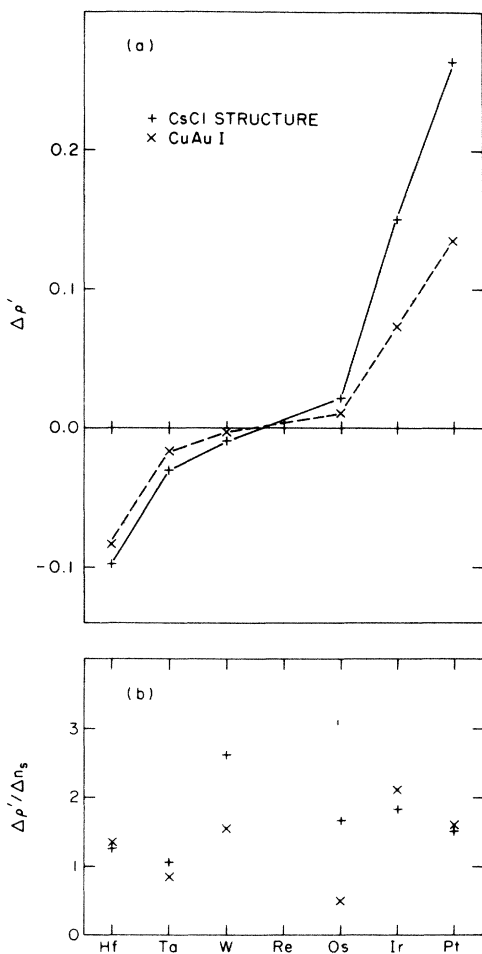


FIG. 9. (a) $\Delta\rho'$, the change in contact density between the alloys and the elemental metals divided by the valence contact density per s electron (as measured by the Wigner-Seitz s populations of the elemental metal). (b) $\Delta\rho'/\Delta n_s$, where Δn_s is the change in Wigner-Seitz s population.

An alternative is to divide $\Delta\rho'$ by the WS cell Δn_s and obtain a ratio which should equal one if the s transfer dominates (i.e., no significant screening of s) in $\rho(0)$ and if the contact density of orbital s character involved in charge transfer equals the contact density, $\Delta\rho_v(0)/n_s$, of the average s -like orbital in the elemental metal. Granted that there is scatter,¹⁶ the ratios so plotted in Fig. 9(b) are significantly above one for all elements but Ta. One might expect that the $\rho(0)$ associated with s charge transfer onto Pt, Ir, and Os is larger than $\rho_v(0)/n_s$ since it is associated with high-lying, hence compact, orbitals. Similarly, to the extent that s transfer off Hf, Ta, and W comes from deep, in energy, in the occupied bands its $\rho(0)$ might be smaller than $\rho_v(0)/n_s$. Hence one might expect ratios somewhat less than one for Hf, Ta, and W accompanied by ratios somewhat above one for the others. The extent to which this is not the case suggests that screening has observably affected the $\Delta\rho(0)$ obtained for these.

VI. CONCLUSION

In summary we have calculated the heat of formation and crystal structure for a series of metallic compounds which are isoelectronic with rhenium, WOs, TaIr, and HfPt. We find that the heats are in reasonable accord with experiment, increasing as Δz , the difference in atomic number of the constituents increases. We also find a crossover from the CuAuI crystal structure to CsCl with Δz which agrees with experiment.

The analogous compounds in the $4d$ row have been studied by Williams *et al.*¹⁷ They have used their results to argue in favor of the d -bond model of compound formation as put forth by Pettifor.¹⁸ The $4d$ compounds MoRu, NbRh, and ZrPd show the same trend as the $5d$'s—increased bonding as Δz increases. However, there is no crossover in crystal structure, the CuAuI structure is favored for all three. MoRu ($\Delta z = 2$) has a negative heat of formation in contrast to WOs which is positive. Also, ZrPd ($\Delta z = 6$) bonds less strongly than HfPt. These differences may be due to the larger bandwidth of the $5d$ elements relative to the $4d$'s.

Heats of formation for the $5d$ compounds treated here have also been calculated by Robbins using an approximate tight-binding theory.¹⁹ His result is in good agreement with ours for HfPt, but he predicts more bonding for the other two compounds.

We have also calculated the change in core-level binding energy relative to the Fermi energy. Simple charge-flow arguments suggest that the element which gains charge should suffer a reduction in core-level binding energy. Of the three compounds studied TaIr fits this picture, but for HfPt and WOs the binding energies of both elements move the same way. This suggests that charge flows cannot readily be inferred from core-level binding-energy shifts.

Finally, we considered the change in contact density as would be obtained from Mössbauer isomer-shift measurements. Here we find that the contact densities do increase for Os, Ir, and Pt in agreement with electronegativity and with the gross Mulliken populations (but not the gross Wigner-Seitz populations). We also find that the change

in s population is insufficient to characterize the change in contact density. Changes in non- s must also be accounted for, indicating the importance of screening effects. Screening effects were found *not* to be important in a recent study of impurities in iron.

We have examined the Mulliken and Wigner-Seitz populations and found that the gross populations disagree on the sign of the charge transfer for the compounds in the CsCl structure. On the other hand, the sum of the s , p , and d populations alone do agree and are consistent with electronegativity arguments that charge flows to the element with the larger Z .

ACKNOWLEDGMENTS

This work was supported by the Division of Materials Sciences, U.S. Department of Energy under Contract No. DE-AC02-76CH00016 and by an allocation of computer time at the National Magnetic Fusion Energy Computer Center at Lawrence Livermore Laboratory.

APPENDIX A

The LASTO method as described in Ref. 2 was used except that it was generalized to handle more than one atom in the unit cell. Therefore, the basis functions in the interstitial region were given by

$$\psi_{inlm}(\mathbf{r}) = \frac{1}{\sqrt{N}} \sum_{\mathbf{R}} e^{i\mathbf{k}\cdot\mathbf{R}} \phi_{nlm}(\mathbf{r} - \mathbf{R} - \tau_i), \quad (\text{A1})$$

where \mathbf{R} labels the unit cell, τ_i the position of the i th atom within the unit cell, and $\phi(\mathbf{r})$ is a Slater-type orbital

$$\phi_{nlm}(\mathbf{r}) = r^{n-1} e^{-\zeta r} Y_{lm}(\mathbf{r}). \quad (\text{A2})$$

The Bloch sum in Eq. (A1) is matched at each sphere boundary onto numerical solutions of the scalar relativistic Dirac equation. Solutions with $l \leq 8$ were used inside the spheres. In practice, the easiest way to effect the matching is to rewrite the Bloch sum, Eq. (A1), in its reciprocal-lattice representation

$$\psi_{inlm}(\mathbf{r}) = \frac{1}{\sqrt{N}} \sum_{\mathbf{g}} e^{i(\mathbf{k}+\mathbf{g})\cdot(\mathbf{r}-\tau_i)} \frac{1}{\Omega} \tilde{\phi}_{nlm}(\mathbf{k}+\mathbf{g}), \quad (\text{A3})$$

where $\tilde{\phi}$ is the Fourier transform of ϕ and Ω is the unit-cell volume. Terms in the sum with $|\mathbf{g}| \leq g_{\text{cut}}$ were included. Typically, g_{cut} was $\sim 8\pi/a$. When using single- ζ basis sets we found that this sum is not completely converged. In fact, the total energy went through a shallow minimum as a function of g_{cut} and these minimum values were used. When the basis set was expanded to a double- ζ basis no such minimum was observed and there were only slight changes in the heat of formation.

The total energy also varies with ζ . The ζ values were chosen to minimize the total energy of the elements. In the course of these calculations we discovered a programming error which changed the optimum ζ 's slightly from those reported previously.² The values we used are given in Table I. The total energies with the new ζ 's were changed only slightly and differences between different structures were unaffected.

APPENDIX B: POPULATION ANALYSIS

If a wave function ψ is given in terms of a set of basis functions $\{\phi_i, i=1, N\}$ by

$$\psi = \sum_i c_i \phi_i, \quad (\text{B1})$$

then the corresponding density is given by

$$\psi^* \psi = \sum_{i,j} c_i^* \phi_i^* \phi_j c_j. \quad (\text{B2})$$

Integrating over all space, we obtain the total charge Q contained in this wave function

$$Q = \sum_{i,j} c_i^* S_{ij} c_j, \quad (\text{B3})$$

where S_{ij} is the overlap of the i th and j th basis functions. Making use of the reality of Q , one can derive the Mulliken populations³ Q_i corresponding to the i th basis function:

$$Q = \sum_i \text{Re} \left[\sum_j c_i^* S_{ij} c_j \right] \equiv \sum_i Q_i, \quad (\text{B4})$$

$$Q_i = \sum_j \text{Re}(c_i^* S_{ij} c_j). \quad (\text{B5})$$

This procedure effectively divides the overlap charge evenly between the two basis functions. A modified Mulliken population analysis⁴ that instead divides the overlap charge in proportion to the diagonal contributions can be obtained easily starting from Eq. (B4)

$$\begin{aligned} Q &= \sum_{i,j} \frac{S_{ii} |c_i|^2 + S_{jj} |c_j|^2}{S_{ii} |c_i|^2 + S_{jj} |c_j|^2} \text{Re}(c_i^* S_{ij} c_j) \\ &= \sum_{i,j} \frac{1}{S_{ii} |c_i|^2 + S_{jj} |c_j|^2} [S_{ii} |c_i|^2 \text{Re}(c_i^* S_{ij} c_j) \\ &\quad + S_{jj} |c_j|^2 \text{Re}(c_i^* S_{ij} c_j)]. \end{aligned}$$

Interchanging i and j in the second term and noting that since $S_{ij} = S_{ji}^*$, one has

TABLE I. Corrections of optimum ζ values previously reported in Ref. 2.

	Hf	Ta	W	Os	Ir	Pt
ζ_{5d}	2.05	2.19	2.40	2.53	2.54	2.58
ζ_{6s}	2.09	2.18	2.29	2.51	2.57	2.64
ζ_{6p}	1.48	1.61	1.70	1.80	1.86	1.93

$$\operatorname{Re}(c_i^* S_{ij} c_j) = \operatorname{Re}(c_j^* S_{ji} c_i), \quad (\text{B6})$$

and hence the total charge can be written as

$$Q = \sum_i \sum_j \frac{2S_{ii} |c_i|^2}{S_{ii} |c_i|^2 + S_{jj} |c_j|^2} \operatorname{Re}(c_i^* S_{ij} c_j) \equiv \sum_i \tilde{Q}_i, \quad (\text{B7})$$

$$\tilde{Q}_i = \sum_j \frac{2S_{ii} |c_i|^2}{S_{ii} |c_i|^2 + S_{jj} |c_j|^2} \operatorname{Re}(c_i^* S_{ij} c_j). \quad (\text{B8})$$

Note that various other population analyses could be derived along the same lines, differing on how one divides the overlap charge between the basis functions. Another approach (e.g., the Löwdin²⁰ population analysis) is to make a transformation to an orthogonal basis and then define the populations in terms of this new set of functions.

¹J. W. Davenport, Phys. Rev. B **29**, 2896 (1984).

²J. W. Davenport, M. Weinert, and R. E. Watson, Phys. Rev. B **32**, 4876 (1985); **32**, 4883 (1985).

³R. S. Mulliken, J. Chem. Phys. **23**, 1833 (1955).

⁴E. W. Stout and P. Politzer, Theor. Chim. Acta **12**, 379 (1968).

⁵D. J. Chadi and M. L. Cohen, Phys. Rev. B **8**, 5747 (1973).

⁶For example, M. J. Monkhorst and J. D. Pack, Phys. Rev. B **13**, 5188 (1976).

⁷R. E. Watson and L. H. Bennett, CALPHAD **8**, 307 (1984).

⁸For a recent tabulation, see C. Colinet, A. Pasturel, and P. Hicter, CALPHAD **9**, 71 (1985).

⁹Calculations were done for the charge residing within Wigner-Seitz spheres rather than within WS cells. In the cases of PtHf and IrTa, where the molecular volumes were somewhat less than the sums of the elemental volumes, the elemental sphere radii, R_{WS} , were multiplied by a *common* factor so that the sum of their volumes equaled that of the compound. Straight sampling of the charge out to R_{WS} yields total electron charge counts which deviate somewhat from the exact integral number of electrons appropriate to the molecular (or elemental) unit. Components of the valence charge residing in the interstitial region, i.e., between R_S and R_{WS} , were normalized by a common factor, for all l in all WS spheres, so as to retrieve the correct integral count.

¹⁰R. E. Watson and L. H. Bennett, Phys. Rev. B **18**, 6439 (1978).

¹¹A similar reversal in the rule for d transfer in calculations for $4d$ - $4d$ alloys has been observed [A. R. Williams (private communication)].

¹²A. DasGupta, P. Oelhafen, U. Gubler, R. Lapka, H. J. Güntherodt, V. L. Moruzzi, and A. R. Williams, Phys. Rev. B **25**, 2160 (1982).

¹³R. E. Watson, J. Hudis, and M. L. Perlman, Phys. Rev. B **4**, 4139 (1971).

¹⁴R. E. Watson, L. J. Swartzendruber, and L. H. Bennett, Phys. Rev. B **24**, 6211 (1981).

¹⁵H. Akai, S. Blügel, R. Zeller, and P. H. Dederichs, Phys. Rev. Lett. **56**, 2407 (1986).

¹⁶There is wide scatter between points for the two crystal structures for W and Os, less for Ta and Ir, and none for Hf and Pt. In large part this is a reflection of the fact that $\Delta\rho(0)$ and Δn_s are small quantities for the former and increase on going to Hf and Pt. A fixed discrepancy in $\Delta\rho(0)$ accompanied by the variation in Δn_s accounts well for the spread.

¹⁷A. R. Williams, C. D. Gelatt, Jr., and V. L. Moruzzi, Phys. Rev. Lett. **44**, 429 (1980).

¹⁸D. G. Pettifor, in *Physical Metallurgy*, 3rd ed., edited by R. W. Cahn and P. Hassen (North-Holland, Amsterdam, 1983), p. 133.

¹⁹M. O. Robbins and L. M. Falicov, Phys. Rev. B **29**, 1333 (1984), and private communication.

²⁰P. O. Löwdin, J. Chem. Phys. **18**, 365 (1950).